Electrical, Control and Communication Engineering
ISSN 2255-9159 (online)
ISSN 2255-9140 (print)
2020, vol. 16, no. 2, pp. 78–87
https://doi.org/10.2478/ecce-2020-0012
https://content.sciendo.com

Effectively Tunable Bandpass Waveguide Filter Based on Incorporation of Coupled Cylindrical Resonators Cut in Half

Karlis Kimsis* (*PhD student, Riga Technical University, Riga, Latvia*)
Janis Semenjako (*Assistant Professor, Riga Technical University, Riga, Latvia*)
Yury V. Shestopalov (*Professor, University of Gävle, Gävle, Sweden*)

Abstract **– A novel mechanically tunable waveguide dielectric filter is presented in this paper. The resonant structure of the filter is made of a rectangular waveguide cavity and an H-plane dielectric cylinder cut in half. The resonating frequency of the proposed structure can be significantly changed by moving two split cylinder parts. The coupling matrix synthesis technique is used to create the required bandpass filter. A drawback of the proposed structure is that the tuning process invokes a mismatch between the feeding structure and the filter. To overcome this drawback, the tuning screws between the coupling irises are used. A filter with the proposed geometry has a large frequency tuning range as well as relatively constant passband bandwidth.**

Keywords **– Bandpass filters; Coupled resonator filters; Dielectric filters; Tuning; Waveguide filters.**

I. Introduction

This article looks at waveguide resonator filters with inductive dielectric cylinders and dielectric in half cylinders, finds out the problems associated with the cylinder permittivity mismatch of the design parameters and a new design effective tunable filter is offered.

Microwave filters are essential components of modern electronics and communication systems operating at microwave frequencies, and their role and applications are only growing [1], [2]. The development of microwave filter technology from an application perspective – military applications, satellite communications, cellular communications base stations, various filters and selective wide-band low-loss tunable waveguide filters required for cellular radio handsets – is essential for this purpose [3].

Microwave filters began to be researched and used more than 80 years ago. There are many studies and publications on the subject of microwave filters of various types and applications used in coaxial lines, waveguides, microstrip lines and as dielectric resonators. In most cases, filter characteristics are selected, such as Chebyshev, elliptic and pseudo-elliptic function, and a variety of generalized designs is used [4]–[7]. In the 1970s, when satellite and other modern communication systems began to develop rapidly, the requirements for microwave filter parameters increased, which gave rise to the development of jet filter synthesis and calculation techniques. During the next decades there were two major advances in filter design: 1) advanced filtering functions incorporating built-in transmission zeros and, as a result, the reflex cross-coupled microwave filter which allowed for inter-resonator couplings between sequentially numbered resonators to be implemented [8]; 2) development of dual-mode technology for waveguide filters which include the development of the coupling matrix method and the propagating dual-mode waveguide configuration [9], [10]. A widely used general method for the synthesis of the folded configuration, coupling matrix for Chebyshev or other filtering functions of the most general type is presented and developed in [11]–[13].

The coupling matrix network synthesis method, its development and application are briefly described in an excellent review [14]. Several modern and widely used methods to design a wide variety of microwave filters in various technologies have been developed in recent decades [15]–[19].

The aforementioned theories and techniques are widely used, as well as specially developed CAD-prone methods. Various CAD methods are used to calculate the microwave filter and optimize its parameters [20]–[22]. The space mapping method is widely used in microwave filter design [23], [24]. Paper [25] reviews the state of the art of the space mapping for modelling and design of engineering devices and systems, e.g., RF and microwave components, and this method is successfully applied in the design of microwave filters. Not only universal software tools for 3D electromagnetic field simulation such as CST and HFSS can be used for filter calculations, but also specialized software directly developed for waveguide filter calculations is offered in [26].

Nowadays, advanced communication systems request for miniaturization and size reduction and, therefore, waveguide filters with dielectric resonators of different shapes and locations are becoming increasingly popular despite the fact that their practical implementation is not convenient. Calculations have been made for filters with dielectric cylinders so that their axes are not parallel to the waveguide wall planes [27], [28]. Easier-to-produce, high-performance waveguide filters with H-plane cylindrical posts are still in widespread use.

* Corresponding author.
E-mail: karlis.kimsis@gmail.com

Waveguide filters with dielectric cylindrical posts can be implemented in different ways and here the use of waveguide dielectric resonator filters is more popular now [29], [30]. Many special H-plane dielectric filter calculation methods have also been developed that provide a solution faster than universal programming tools [31]–[33], which is especially important when looking at filters reacting to changes in the dielectric resonator parameters used in their design.

However, none of the above-mentioned publications and many others give an analysis of the variations in the design parameters of the filters if the actual permittivity of the dielectric cylinders differs from the assumed one despite the fact that the dielectric product manufacturers allow for uncertainty in the permittivity values [34], [35].

However, calculations and experiments carried out show that even relatively small uncertainty in the permittivity values makes a significant difference between the calculated and real (experimentally measured) filter characteristics. This fact is also recorded in the article [36] which states that "the measured response of Chebyshev ceramic waveguide filter designed in Section 4 needs tuning to mitigate the effects of material discrepancies and physical dimension tolerances". The article [37] clearly states that "designers should always think about minimizing production labour, considering manufacturing tolerances possibly as a trade-off against tuning time and recognizing that availability of skilled labour is more than simply a cost but rather a constraint on delivery rate".

It has to be concluded that a filter without the intended turning and matching capabilities is only theoretically good, but will not be used in practice.

Tuning filters and tuning methods are offered and implemented and tuning screws are commonly used as tuning elements [2], [21], [38].

Each tuning screw affects not only the element value it is supposed to, but also the all network elements nearby and the optimal and effective tuning must be carefully calculated [39]. In fact, many manufacturers offer customizable filters, but tuning the filters requires good professional skills [40], [41] and more accurate manufacture of a microwave filter is more than desired, but it is very expensive and often impracticable, as well as the tuning process is time consuming and inexpensive [42].

The procedures offered for accurate tuning of the filters are mainly based on tuning screws, which are, as a rule, computer-aided, complicated [42]–[44] and there is no further information on their application. The tuning procedures are described in detail only in article [24], and the proposed procedure are also applicable to any microwave filter that includes tuning elements.

This article presents a new design of the tunable waveguide filter with half-slit H-plane dielectric cylinders, which are placed as shown in Fig. 1a. The resonance frequency of split cylinders varies within a relatively wide range, if the distance between the half-cylinders is changed, which was reported in [45] and that is why a filter cell with two half-cylinder resonators (HCR) was chosen as the prototype of a tunable filter.

The design of such a HCR filter was chosen because calculations showed that a filter made of cylindrical resonators (Fig. 1a) could not be adjusted if the permittivity of the dielectric cylinders deviated from the nominal value limit specified by the manufacturer and assumed in the filter calculations.

In the proposed design, the main tuning is done by changing the geometric dimensions of the dielectric resonators (distance between the half-cylinders) and the tuning screws are an additional alignment element that provides the alignment of better matching.

The design of the filter proposed here allows the filter tuning to be carried out over a much wider range of parameters compared to traditional methods with only tuning screws, which are often insufficient when the permeability of the dielectric portions of the filter differs from the estimated one, which is a common practice.

II. Dielectric Resonator

In the first step, the filter with dielectric cylinder resonators [22] with permittivity ε_r = 10.0 (Fig. 1a) was designed. The filter parameters were chosen as follows: filter order N = 4; centre frequency $f_0 = 1.86$ GHz, and fractional bandwidth FBW = 1 %. The N+2 coupling matrix method [12] was used, and all the parameters were found using eigenmode solver provided by CST Studio Suite and the methodology described in [1]. It was found that if the actual permittivity of the dielectric cylinders differed in a relatively small range, for example, $\varepsilon_r = 10.0 \pm 0.3$ the centre frequency changes would be unacceptable. However, it must be respected that the dielectric product manufacturers allow for uncertainty in the permittivity values [34], [35], and this circumstance must be taken into account in the filter design. The widespread method of tuning such filters using tuning screws [2], [43] failed to match this filter to the selected f_0 .

To obtain additional tuning capabilities instead of using a cylinder as a resonating element, we investigated the additional capabilities of a filter whose dielectric resonators were formed from half-split dielectric cylinders (HSC) arranged as shown in Fig. 1b.

Calculation of the resonator from HSC shows the resonating frequency of the waveguide TE_{10} mode for different distance s between half-cylinders, permittivity of cylinder halves and radius of cylinder halves (Fig. 2 and Fig. 3). In calculations, the cavity dimensions chosen are 50.8 mm × 51.5 mm × 50.8 mm, designed radius of the cylindrical halves r was accepted r = 10.0 mm and relative dielectric permittivity ε_r = 10.0.

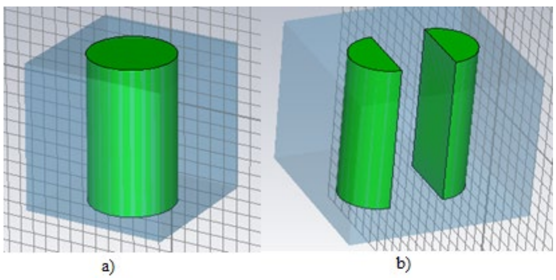

Fig. 1. Conventional dielectric cylinder resonator structure (a) and half-split dielectric cylinder resonator structure (b).

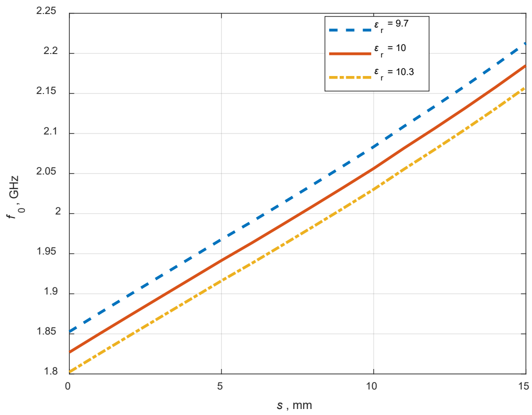

Fig. 2. Resonant frequency of TE_{10} mode as a function of separation between half-cylinders for different relative dielectric permittivity of cylinder.

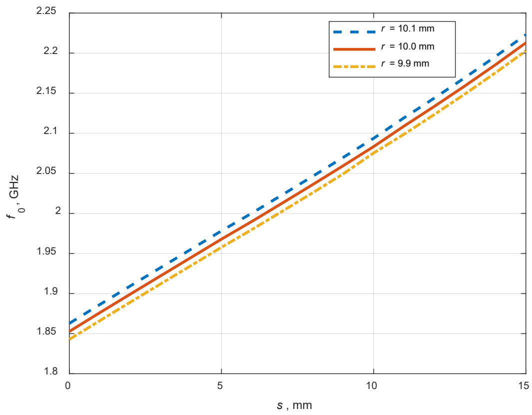

Fig. 3. Resonant frequency of TE_{10} mode as a function of separation between half-cylinders for different radius of the cylinder.

As it is shown in Fig. 2 and 3, the change in resonant frequency of the filter cavity introduced by a small change in design parameters (a manufacturing error) would be damaging in a final filter design. Figures 2 and 3 also show that the design with HSC makes possible to tune the cavity to a different resonating frequency by changing the distance between cylinder halves *S*.

In this paper, the HSC dielectric filter system is proposed to create a tunable bandpass filter, in which the filter bandpass frequency can be adjusted by changing the distance between the cylinder halves s because such a design makes it possible to change the resonant frequency within a relatively large range.

III. Filter Design

In order to test our assumption about the possibility of creating a tunable bandpass filter, we calculated a narrowband coupled resonator bandpass filter employing split cylinder resonators.

The filter was designed based on the *N*+2 coupling matrix method [12], and all the necessary parameters were found using Eigenmode solver provided by CST Studio Suite and the methodology described in [1].

Next a brief outline of the *N*+2 coupling matrix synthesis procedure will be given. The synthesis procedure is based on the fact that the transfer and reflection functions of the filter can be expressed as a ratio of two *N*-th degree polynomials

$$S_{11}(\omega) = \frac{F_N(\omega)}{E_N(\omega)} \tag{1}$$

$$S_{21}(\omega) = \frac{P_N(\omega)}{\alpha E_N(\omega)}, \tag{2}$$

where ω is the real frequency variable related to the complex frequency variable $S = j\omega$, N is the filter order and α is a constant normalizing S_{21} to unity

$$\alpha = \frac{1}{\sqrt{10^{RL/10}-1}} \left.\frac{P_N(\omega)}{F_N(\omega)}\right|_{\omega=1}, \tag{3}$$

where RL is the prescribed return loss of the filter.

Polynomial $P_N(\omega)$ contains transmission zeros if there are any. In our work, we employ symmetrical filtering networks, so polynomial $P_N(\omega) = 1$.

From Eqs. (1) and (2) it is seen that $S_{11}(\omega)$ and $S_{21}(\omega)$ share a common denominator polynomial. Using the law of conservation of energy for a lossless network $S_{11}^2(\omega) + S_{21}^2(\omega) = 1$ it is possible to derive an expression for one of the scattering parameters

$$S_{21}(\omega) = \frac{1}{1+\alpha^2 C_N^2(\omega)}, \tag{4}$$

where $C_N(\omega) = \dfrac{F_N(\omega)}{P_N(\omega)}$ is the filtering function in the form of Chebyshev polynomial

$$C_N(\omega) = \cosh\left(\sum_{n=1}^{N} \cosh^{-1}(x_n)\right), \tag{5}$$

$$x_n = \frac{\omega - 1/\omega_n}{1-\omega/\omega_n}, \tag{6}$$

where ω_n is the position of the nth transmission zero. Since we are only concerned about the pass filter, all transmission zeros are placed at infinity $\omega_n \to \infty$. Next task is to find the polynomial coefficients for polynomials $F_N(\omega)$ and $E_N(\omega)$. This can be done by employing a recursive technique described in detail in [11].

Next step in generating the *N*+2 coupling matrix is the derivation of the admittance matrix Y_N for the filtering network described by scattering parameters (1) and (2).

$$Y_N = \begin{bmatrix} y_{11}(s) & y_{12}(s) \\ y_{21}(s) & y_{22}(s) \end{bmatrix} = \frac{1}{y_d(s)} \begin{bmatrix} y_{11n}(s) & y_{12n}(s) \\ y_{21n}(s) & y_{22n}(s) \end{bmatrix}, \tag{7}$$

where the term $y_d(\omega)$ is a common denominator for all the $y_{ij}(s)$ terms.

Admittance matrix can be derived directly from the transfer and reflection polynomials (1) and (2) as follows.

For N even

$$y_{21}(s) = \frac{y_{21n}(s)}{y_d(s)} = \frac{P(s)/\alpha}{m_1(s)} \tag{8a^e}$$

$$y_{22}(s) = \frac{y_{22n}(s)}{y_d(s)} = \frac{m_1(s)}{n_1(s)} \qquad (8\mathrm{b^e})$$

For N odd

$$y_{21}(s) = \frac{y_{21n}(s)}{y_d(s)} = \frac{P(s)/\alpha}{n_1(s)} \qquad (8\mathrm{a^o})$$

$$y_{22}(s) = \frac{y_{22n}(s)}{y_d(s)} = \frac{n_1(s)}{m_1(s)}, \qquad (8\mathrm{b^o})$$

where

$$\begin{aligned} m_1(s) &= \mathrm{Re}(e_0 + f_0) + \mathrm{jIm}(e_1 + f_1)s + \mathrm{Re}(e_2 + f_2)s^2 + \ldots \\ n_1(s) &= \mathrm{j\,Im}(e_0 + f_0) + \mathrm{jRe}(e_1 + f_1)s + \mathrm{j\,Im}(e_2 + f_2)s^2 + \ldots \end{aligned} \qquad (9)$$

e_i and f_i, $i = 0, 1, 2, 3, \ldots, N$ are the complex coefficients of $E(s)$ and $F(s)$ polynomials, respectively.

Now the residues r_{21k} and r_{22k} $k = 0, 1, 2, 3, \ldots, N$ of polynomials $y_{21}(s)$ and $y_{22}(s)$ can be found with the partial fraction expansion and the eigenvalues λ_k of the filtering network obtained by rooting the denominator polynomial $y_d(s)$ [12]. Expressing this in matrix form yields the following expression for the admittance matrix

$$Y_N = \mathrm{j}\begin{bmatrix} 0 & K_0 \\ K_0 & 0 \end{bmatrix} + \sum_{k=1}^{N} \frac{1}{(s - \mathrm{j}\lambda_k)} \begin{bmatrix} r_{11k} & r_{12k} \\ r_{21k} & r_{22k} \end{bmatrix}, \qquad (10)$$

where the constant $K_0 = 0$ except for the case when the filter order is equal to the number of transmission zeros.

Now the admittance matrix is known, the synthesis of N+2 coupling matrix can begin. The general N+2 coupling matrix comes in the form of Table I.

TABLE I
GENERAL N+2 COUPLING MATRIX

	S	1	2	…	k	…	N	L
S		M_{S1}	M_{S2}		M_{Sk}		M_{SN}	M_{SL}
1	M_{1S}	M_{11}						M_{1L}
2	M_{2S}		M_{22}					M_{2L}
…				…				…
k	M_{kS}				M_{kk}			M_{kL}
…	…					…		…
N	M_{NS}						M_{NN}	M_{NL}
L	M_{LS}	M_{L1}	M_{L2}	…	M_{Lk}	…	M_{LN}	

where S – source, L – load, M_{SL} – source–load coupling, $M_{Lk} = M_{kL}$, $M_{Sk} = M_{kS} (k = 1, 2, \ldots, N)$, $M_{kk} = -\lambda_k$, $M_{Lk} = \sqrt{r_{22k}}$, $M_{Sk} = \dfrac{r_{21k}}{M_{Lk}}$.

Since every coupling matrix entry describes a physical coupling between source–load, source/load–resonator or resonator–resonator, this matrix representation is very impractical for real life applications because the physical filter would have to have geometry that realizes all the necessary couplings. To overcome this drawback, a number of similarity transforms can be employed to transform the coupling matrix into folded form as detailed in [11].

The folded form representation is much more convenient for physical filter realization since it utilizes a minimal number of coupling elements in order to achieve the necessary scattering parameters.

Next the calculation of microwave filter with HSC resonators is outlined. The filter parameters were chosen as follows: filter order N = 4; centre frequency $f_0 = 1.86$ GHz, fractional bandwidth FBW = 1 %. The relative dielectric permittivity of the resonators was chosen to be ε_r = 10.0.

In order to design the proposed filter using CST, first the filter cavity dimensions need to be chosen as well as the separation between cylinder halves. Then the resonating frequency of the filter cavity needs to be calculated as a function of cylinder radius (Fig. 4). Finally, the radius of the cylinder halves is chosen so that the cavity resonates at the centre frequency of filter passband.

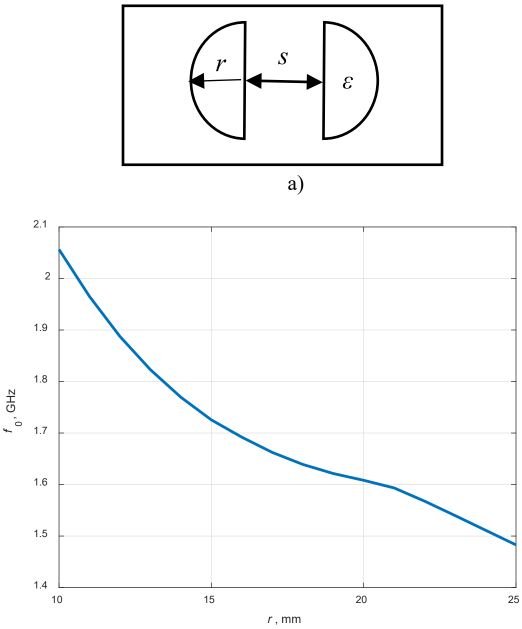

a)

b)

Fig. 4. Filter cavity (a) and its resonant as a function of cylinder radius. ε_r = 10.0, s = 10 mm and waveguide cavity dimensions are 50.8 mm × 51.5 mm × 50.8 mm.

After that the input/output coupling $Q_{\mathrm{ex}} = \dfrac{1}{FBW \cdot M_{1S}^2}$ needs to be determined. We chose to use the coaxial feeding probe in order to excite the filter as shown in Fig. 5. The calculations were made by choosing the probe location p_x and p_y and adjusting the probe depth h_p until we obtained the desired Q_{ex}.

Finally, we need to find the coupling coefficients between adjacent resonators. In order to introduce coupling between resonators, a coupling iris of thickness t and with w is inserted between resonators as shown in Fig. 6. Then the coupling coefficients are calculated using Eigenmode solver and equation $k = \dfrac{f_m^2 - f_e^2}{f_m^2 + f_e^2}$ by changing the widths of the coupling irises until the needed coupling coefficients are found based on the synthesized coupling matrix. Frequencies f_m and f_e correspond to resonating frequencies of resonators as shown in Fig. 6a.

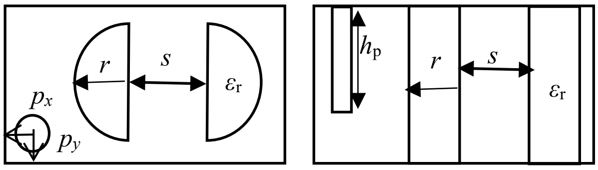

a)

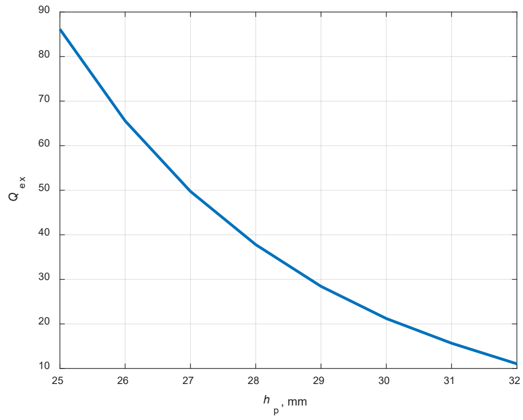

b)

Fig. 5. Geometry used to determine Q_{ex} (a) and its value as a function of coaxial feeding probe depth. Coaxial probe is located at p_x = 10.54 mm, p_y = 10.54 mm.

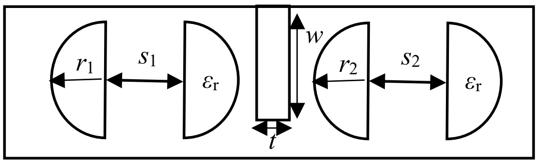

a)

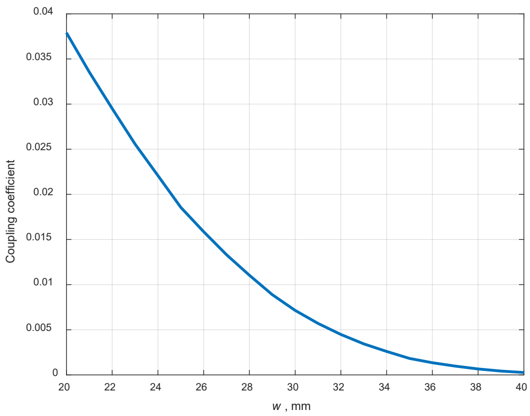

b)

Fig. 6. Geometry used to determine coupling coefficients (a) and coupling coefficients of the filter cavity as a function of iris with w. Iris thickness t = 3.81 mm.

After choosing the right filter dimensions, we optimized the filter using CST trust region optimization scheme. Final filter geometry is shown in Fig. 7 with values listed in Table II. Filter S-parameters are shown in Fig. 8.

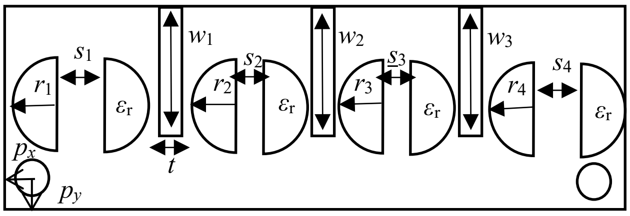

Fig. 7. The proposed filter geometry.

TABLE II
DIMENSIONS FOR THE FILTER, OPTIMIZED WITH CST TRUST REGION SCHEME

Cavity dimensions, mm	50.8 × 51.5 × 50.8
$r_1 = r_4$, mm	11.63
$r_2 = r_3$, mm	11.82
$s_1 = s_2 = s_3 = s_4$, mm	10.00
$w_1 = w_2$, mm	26.93
w_3, mm	28.52
ε_r	10.00
p_x, mm	10.54
p_y, mm	10.54
h_p, mm	26.89

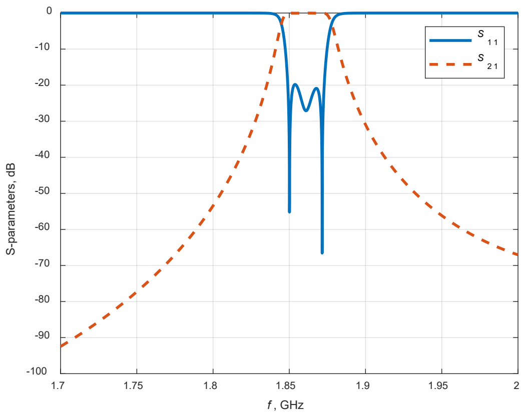

Fig. 8. S-parameters of the proposed filter.

Next we checked what would happen if the relative dielectric permittivity of the resonators was shifted within the margin of error claimed by the manufacturers [34], [35]. We took the original filter design (Figs. 7 and 8) and changed the relative dielectric permittivity of the resonators by +/− 10 % and +/− 1 %.

Figure 9a shows the original filter reflection loss when $\varepsilon_r = 10.0$ as well as the reflection loss of the filter when the relative dielectric permittivity is changed by +/− 10 %. Figure 9b shows the same thing, only the relative dielectric permittivity shift is +/− 1 %.

From Fig. 9a we see that the filter passband has shifted by more than 100 MHz, which is unacceptable in real world applications. In Fig. 9b, the shift is substantially smaller, but still the frequency shift would render this filter unusable.

Next, we examined what would happen when the distance between the cylindrical parts was changed. In the original design (Fig. 7), we chose a constant distance between the cylinders equal to 10 mm. In Fig. 10, we show S_{11} when changing this distance.

As Fig. 10 suggests, this type of structure offers a large tuning bandwidth as well as a relatively constant filter bandwidth, which is desirable in many filter applications. A drawback of this type of structure is that the tuning process invokes a mismatch between the feeding structure and the filter. To overcome this drawback, an additional tuning mechanism needs to be introduced.

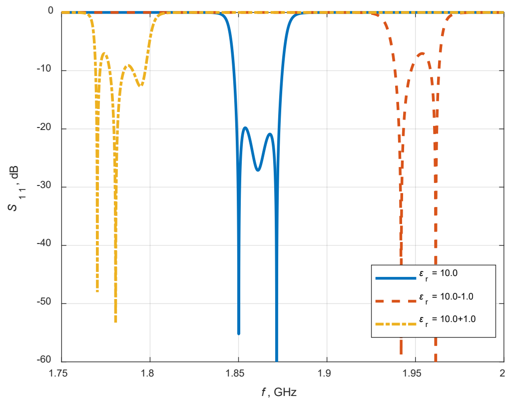

a)

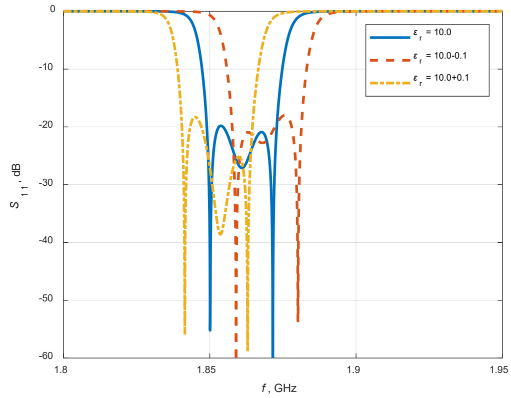

b)

Fig. 9. *S*-parameters of the proposed filter with Δε = +/− 10% from the original value (a) and *S*-parameters of the proposed filter with Δε = +/− 1 % from the original value (b).

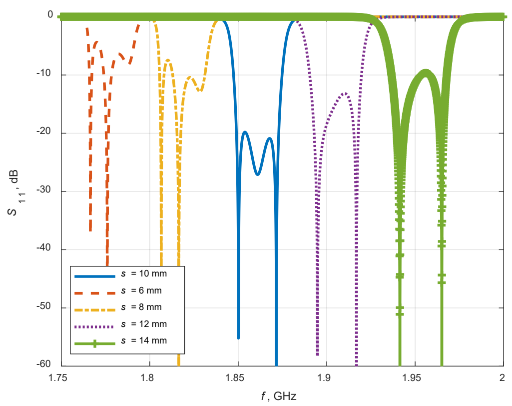

Fig. 10. *S*-parameters of the proposed filter for different distances between the cylinders.

To accomplish this task, we decided to introduce tuning screws between the coupling irises as shown in Fig. 11. The screws were inserted in the middle of all the gaps between the waveguide wall and the coupling irises. The screw diameters were chosen equal to coupling iris thickness t.

Figure 12 shows the coupling coefficient as a function of the tuning screw depth h_s, for different distances between the cylinders.

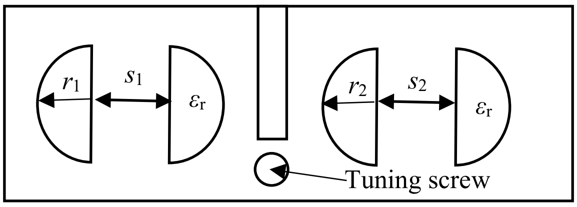

Fig. 11. Tuning screws for coupling coefficient adjustment.

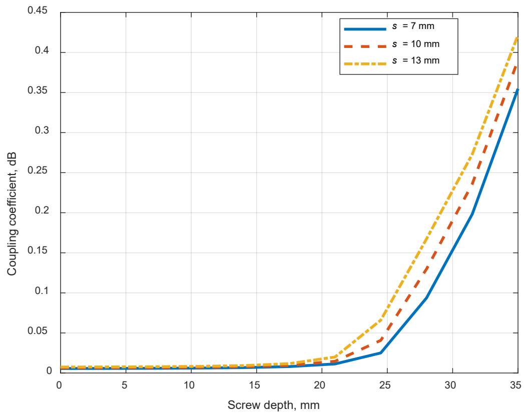

Fig. 12. Coupling coefficient as a function of the tuning screw depth.

As the graph suggests, it is possible to change the coupling coefficient between the resonators by changing the depth of the tuning screws. It is worth noting that a change in coupling coefficient values starts to occur at certain depths of the tuning screws, so it is important to select an appropriate starting depth when designing the first iteration of the filter.

Then we checked how the tuning screws would affect the resonating frequency of the filter cavities as well as the external quality factor Q_{ex} of the feeding structure. To check the impact on the resonating frequency, we created filter cavity shown in Fig. 13. One of the tuning screw depth in Fig. 13 was constant while we changed the depth of the other screw. Figure 14 shows the resonating frequency of TE_{10} mode when changing the depth of one of the tuning screws for different distances between cylinders.

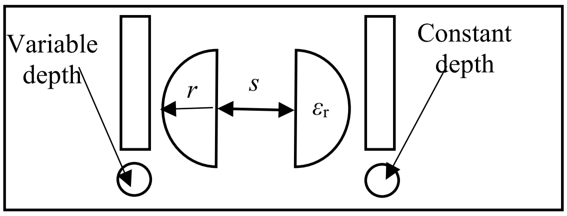

Fig. 13. The model used for estimating the resonant frequency in presence of tuning screws.

From Fig. 14 we can conclude that, by changing the depth of the tuning screws, we change not only the coupling coefficients but also the resonating frequency. It means that in order to tune and match the proposed filter to the desired centre frequency we have to adjust the spacing between the cylinders and the depth of the tuning screws simultaneously to achieve the best filter performance.

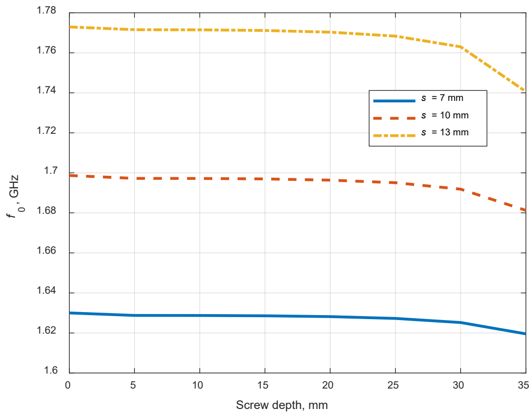

Fig. 14. Tuning screw impact on the resonant frequency for TE_{10} mode.

The impact on the filter Q_{ex} when changing the screw depth was examined using the filter cavity as shown in Fig. 15. The results are plotted in Fig. 16.

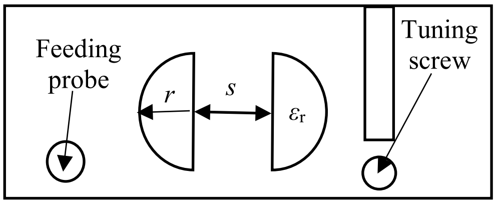

Fig. 15. The model used for estimating Q_{ex} in presence of tuning screws.

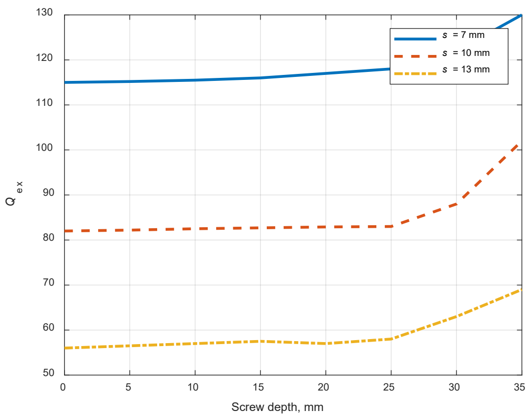

Fig. 16. Tuning screw impact on Q_{ex} for TE_{10} mode.

We can see that when the screw depth gets large enough, the Q_{ex} starts to change, which means that the proposed tuning mechanism can be used to change the filter bandwidth if necessary.

IV. Final Filter Evaluation

In this chapter, we demonstrate the performance of the proposed filter. We had to redesign the original filter shown in Fig. 7 in order to account for the tuning screws. The new filter is shown in Fig. 17. For the initial filter design we set a constant distance between the cylinders. Then by using the coupling matrix method and CST Eigenmode solver as well as optimization, we found the necessary cylinder radiuses, tuning screw depths and coupling iris widths to get the desired filtering function as shown in Fig. 18. The physical parameters of the filter are listed in Table III.

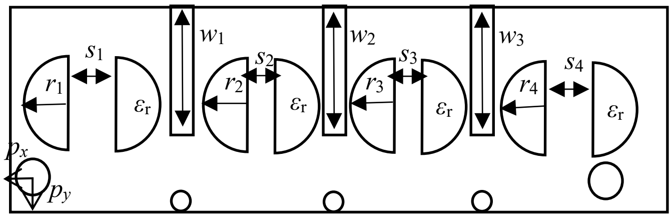

Fig. 17. Geometry of the proposed filter with tuning screws.

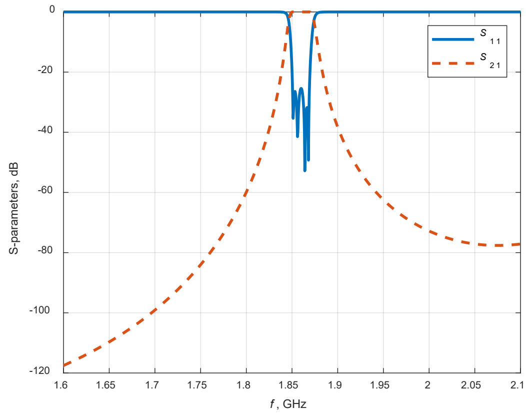

Fig. 18. *S*-parameters for the filter with tuning screws.

TABLE III
DIMENSIONS FOR THE FILTER, CONSIDERING TUNING SCREWS

Cavity dimensions, mm	50.8 × 51.5 × 50.8
$r_1 = r_4$, mm	11.8
$r_2 = r_3$, mm	11.94
s, mm	10.00
$w_1 = w_2$, mm	21.00
w_3, mm	19.89
h_{s1}, mm	24.30
h_{s2}, mm	22.29
h_{s3}, mm	24.30
p_x, mm	10.54
p_y, mm	10.54
h_p, mm	26.84
ε_r	10.00

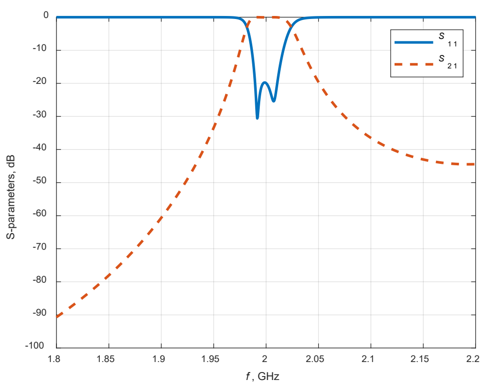

Fig. 19. *S*-parameters of the proposed filter with the centre frequency tuned to 2 GHz.

Next, we checked if it was possible to tune this filter to a different centre frequency by changing only the distance between the cylinders and tuning screw depths. Figures 19 and 20 show the optimized *S*-parameters when the filter is tuned to 2 GHz and 1.8 GHz centre frequency by adjusting the distances between half-cylinders and the depths of the tuning screws, which are listed in Tables IV and V.

TABLE IV
DIMENSIONS FOR THE FILTER WITH THE CENTRE FREQUENCY TUNED TO 2 GHZ

s_1, mm	16.30
s_2, mm	16.09
s_3, mm	16.06
s_4, mm	16.39
h_{s1}, mm	26.70
h_{s2}, mm	24.20
h_{s3}, mm	26.67

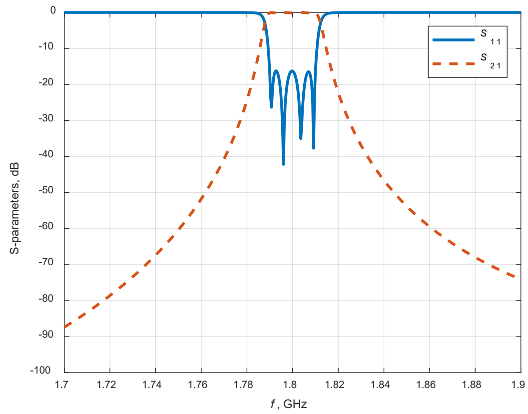

Fig. 20. *S*-parameters of the proposed filter with the centre frequency tuned to 1.8 GHz.

TABLE V
DIMENSIONS FOR THE FILTER WITH THE CENTRE FREQUENCY TUNED TO 1.8 GHZ

s_1, mm	7.14
s_2, mm	7.24
s_3, mm	7.24
s_4, mm	7.14
h_{s1}, mm	24.12
h_{s2}, mm	23.30
h_{s2}, mm	23.86

Then we checked what would happen if the relative dielectric permittivity of the resonators was shifted within the margin of error claimed by the manufacturers [34], [35]. We took the filter design shown in Figs. 17 and 18 and changed the relative dielectric permittivity of the resonators by Δε = +/− 3 % from the original value.

Figure 21 shows the original filter reflection loss when the relative dielectric permittivity is ε_r = 10.0 as well as the reflection loss of the filter when the relative dielectric permittivity is changed to $\varepsilon_r + \Delta\varepsilon$ and $\varepsilon_r - \Delta\varepsilon$.

We can see that a 3 % error in relative dielectric permittivity introduces an unacceptable frequency shift of the filter passband. This frequency shift can be compensated by adjusting the distances between the cylinders and tuning screw depths.

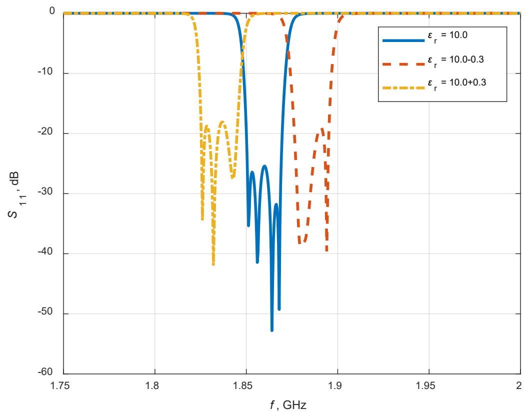

Fig. 21. *S*-parameters of the proposed filter for different relative dielectric permittivity of the resonators.

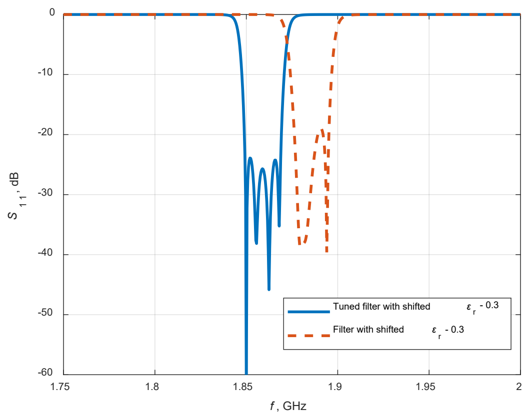

Fig. 22. *S*-parameters for the case when the relative dielectric permittivity of the resonators is changed by −3 %.

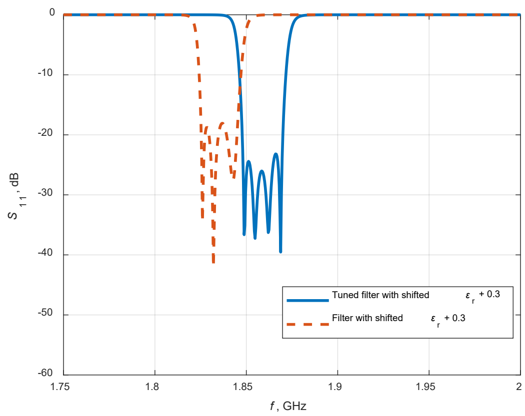

Fig. 23. *S*-parameters for the case when the relative dielectric permittivity of the resonators is changed by +3 %.

The results are shown in Figs. 22 and 23, where Fig. 22 shows the filter when the relative dielectric permittivity is lowered by 3 % and the filter is tuned to resonate at its original centre frequency, and Fig. 23 shows the same for the case when the relative dielectric permittivity is increased by 3 %. The distances between half-cylinders and the depths of the tuning screws are listed in Tables VI and VII, respectively.

TABLE VI
DIMENSIONS FOR THE FILTER WITH RELATIVE DIELECTRIC PERMITTIVITY LOWERED BY 3%

s_1, mm	8.85
s_2, mm	8.85
s_3, mm	8.857
s_4, mm	8.868
h_{s1}, mm	24.80
h_{s2}, mm	23.66
h_{s3}, mm	24.77

TABLE VII
DIMENSIONS FOR THE FILTER WITH RELATIVE DIELECTRIC PERMITTIVITY INCREASED BY 3%

s_1, mm	11.08
s_2, mm	11.07
s_3, mm	11.07
s_4, mm	11.11
h_{s1}, mm	24.67
h_{s2}, mm	23.83
h_{s3}, mm	24.67

V. CONCLUSION

In this paper, we have proposed the new geometric shape waveguide dielectric resonators – half-split dielectric cylinders with parallel slit planes. It has been shown that distance reduction between split planes allows for efficient adjustment of filters over a wide range of possible manufacturing errors.

The tuning screws in this filter are used only as an additional element that provides the alignment of better matching. The design of the filter proposed here allows the filter tuning to be carried out over a much wider range of parameters compared to traditional methods with only tuning screws.

Although the study has found evidence that split dielectric resonators in waveguide filters ensure effective filter alignment, such a design requires a precise additional device for tuning. In the future it is intended to study dielectric resonators, in which the resonant frequency is changed by rotating one of the resonator parts relative to the other.

REFERENCES

[1] J. S. Hong, M. J. Lancaster, Microstrip Filters for RF/Microwave Applications. New York: John Wiley & Sons, INC, 2001. ttps://doi.org/10.1002/0471221619

[2] R. J. Cameron, C. M. Kudsia, and R. R. Mansour, Microwave Filters for Communication Systems: Fundamentals, Design and Applications (2nd ed.). New Jersy: John Wiley, Sons; Inc. Hoboken, 2018. https://doi.org/10.1002/9781119292371

[3] I. C. Hunter, L. Billonet, B. Jarry, and P. Guillon, "Microwave filters-applications and technology," *IEEE Transactions on Microwave Theory and Techniques*, vol. 50, no.3, pp. 794–805, March 2002. https://doi.org/10.1109/22.989963

[4] G. L. Matthaei, L. Young L, and E. M. T. Jones. Microwave filters, impedance-matching networks, and coupling structures. North Belgin, NJ, USA: McGraw-Hill; 1964. https://doi.org/10.21236/AD0402930

[5] S. B. Cohn, "Microwave Bandpass Filters Containing High-Q Dielectric Resonators," *IEEE Transactions on Microwave Theory and Techniques*, vol.16, no.4, pp. 218–227, Apr. 1968. https://doi.org/10.1109/TMTT.1968.1126654

[6] B. Yu. Kapilevich. Waveguide Dielectric Filters. USA: Springfield, International Translation Company, NTIS, 1981 (translated from Russian by K. B. Howe, Moskva, Sviaz, 1980).

[7] R. Levy and S. B. Cohn, "A History of Microwave Filter Research, Design, and Development," *IEEE Transactions on Microwave Theory and Techniques,* vol. 32, no. 9, pp. 1055–1067, Sep. 1984. https://doi.org/10.1109/TMTT.1984.1132817

[8] J. D. Rhodes, "The generalized direct-coupled cavity linear phase filter," *IEEE Trans. Microwave Theory Tech.*, vol. 18, no. 6, pp. 308–313, Jun. 1970. https://doi.org/10.1109/TMTT.1970.1127224

[9] A. E. Atia and A. E. Williams, "Narrow-Bandpass Waveguide Filters," *IEEE Transactions on Microwave Theory and Techniques,* vol. 20, no.4, pp. 258–265. Apr. 1972. https://doi.org/10.1109/TMTT.1972.1127732

[10] A. E. Atia, A. E. Williams, and R. W. Newcomb, "Narrow-band multiple-coupled cavity synthesis," *IEEE Trans. Circuits Syst.*, vol. 21, no. 5, pp. 649–655, Sep. 1974. https://doi.org/10.1109/TCS.1974.1083913

[11] R. J. Cameron, "General coupling matrix synthesis methods for Chebyshev filtering functions," *IEEE Trans. Microwave Theory Tech.*, vol. 47, no. 4, pp. 433–442, Apr. 1999. https://doi.org/10.1109/22.754877

[12] R. J. Cameron, "Advanced coupling matrix synthesis techniques for microwave filters," *IEEE Trans. Microwave Theory Tech.*, vol. 51, no. 1, pp. 1–10, Jan. 2003. https://doi.org/10.1109/TMTT.2002.806937

[13] R. J. Cameron, C. M. Kudsia, and R. R. Mansour, Microwave Filters for Communication Systems, Fundamentals, Design and Applications. New York: Wiley, 2007.

[14] R. J. Cameron, "Advanced Filter Synthesis," *IEEE Microwave Magazine,* vol. 12, no.6, pp. 42–61, Oct. 2011. https://doi.org/10.1109/MMM.2011.942007

[15] R. Levy, R.V. Snyder, and G. Matthaei, "Design of microwave filters," *IEEE Transactions on Microwave Theory and Techniques,* vol. 50, no. 3, pp. 783–793, Mar. 2002. https://doi.org/10.1109/22.989962

[16] C. Bachiller, H. E. Gonzalez, V. E. B. Esbert, A.B. Martinez, and J.V. Morro, "Efficient Technique for the Cascade Connection of Multiple Two-Port Scattering Matrices," *IEEE Transactions on Microwave Theory and Techniques*, vol. 55, no. 9, pp. 1880–1886, Sept. 2007. https://doi.org/10.1109/TMTT.2007.904076

[17] S. Bastioli, C. Tomassoni, and R. Sorrentino, "A New Class of Waveguide Dual-Mode Filters Using TM and Nonresonating Modes," *IEEE Transactions on Microwave Theory and Techniques,* vol. 58, no. 12, Dec. 2010. https://doi.org/10.1109/TMTT.2010.2086068

[18] C. Tomassoni, S. Bastioli, and R Sorrentino, "Generalized TM Dual-Mode Cavity Filters," *IEEE Transactions on Microwave Theory and Techniques,* vol. 59, no. 12, pp. 3338–3346. Dec. 2011. https://doi.org/10.1109/TMTT.2011.2172622

[19] Q.-X. Chu, X. Ouyang, H. Wang, and F.-C. Chen, "TE_{01delta}-Mode Dielectric-Resonator Filters With Controllable Transmission Zeros," *IEEE Transactions on Microwave Theory and Techniques*, vol. 61, no. 3, pp. 1086–1094, Mar. 2013. https://doi.org/10.1109/TMTT.2013.2238551

[20] I. D. Robertson, D. Sanchez-Hernandez, and U. Karacaoglu, "CAD techniques for microwave circuits," *Electronics & Communication Engineering Journal*, vol. 8, no. 6, pp. 245–256, Dec.1996. https://doi.org/10.1049/ecej:19960601

[21] V. E. Boria, M. Guglielmi, and P. Arcioni, "Computer-aided design of inductively coupled rectangular waveguide filters including tuning elements," *International Journal of RF and Microwave Computer-Aided Engineering*, vol. 8 no. 3, pp. 226–235, May 1998. https://doi.org/10.1002/(SICI)1099-047X(199805)8:3<226::AID-MMCE6>3.0.CO;2-H

[22] C. Bachiller, H. Esteban, V. E. Boria, J. V. Morro, L. J. Rogla, M. Taroncher, A. Belenguer. "Efficient CAD tool of direct-coupled-cavities filters with dielectric resonators," *2005 IEEE Antennas and Propagation Society International Symposium*. IEEE, Washington, DC, USA, pp. 578–581, July 2005. https://doi.org/10.1109/APS.2005.1551624

[23] J. V. M. Ros, P. S. Pacheco, H. E. Gonzalez, V. E. B. Esbert, C. B. Martin, M. T. Calduch, and B. G. Martinez, "Fast automated design of waveguide filters using aggressive space mapping with a new segmentation strategy and a hybrid optimization algorithm," *IEEE Transactions on Microwave Theory and Techniques*, vol. 53, no. 4, pp. 1130–1142, Apr. 2005. https://doi.org/10.1109/TMTT.2005.845685

[24] J. C. Melgarejo, J. Ossorio, S. Cogollos, M. Guglielmi, V. E. Boria, and J. W. Bandler, "On Space Mapping Techniques for Microwave Filter Tuning," *IEEE Transactions on Microwave Theory and Techniques,* vol. 67, no. 12, 2019, pp. 4860–4870. https://doi.org/10.1109/TMTT.2019.2944361

[25] J. W. Bandler, Q. S. Cheng, S. A. Dakroury, A. S. Mohamed, M. H. Bakr, K. Madsen, and J. Sondergaard, "Space Mapping: The State of the Art," *IEEE Transactions on Microwave Theory and Techniques*, vol. 52, no. 1, pp. 337–361, Jan. 2004. https://doi.org/10.1109/TMTT.2003.820904

[26] WASP NET's wide application range for accurate, fast EM CAD and optimization of all kinds of passive microwave components [Online]. Available: http://www.mig-germany.com/seite18.html [Accessed Nov. 10. 2019].

[27] S. Bastioli and R. V. Snyder, "Inline Pseudoelliptic TE_{01delta}-Mode Dielectric Resonator Filters Using Multiple Evanescent Modes to Selectively Bypass Orthogonal Resonators," *IEEE Transactions on Microwave Theory and Techniques*, vol. 60, no. 12, pp. 3988–4001, Dec. 2012. https://doi.org/10.1109/TMTT.2012.2222659

[28] C. Tomassoni, S. Bastioli, and R. V. Snyder, R. V. "Propagating Waveguide Filters Using Dielectric Resonators," *IEEE Transactions on Microwave Theory and Techniques*, vol. 63, no. 12, pp. 4366–4375, Dec. 2015. https://doi.org/10.1109/TMTT.2015.2495284

[29] C. Bachiller, H. Esteban, J. V. Morro, and V. Boria, "Hybrid mode matching method for the efficient analysis of rods in waveguided structures," *Mathematical and Computer Modelling*, vol. 57, no. 7-8, pp. 1832–1839, Apr. 2013. https://doi.org/10.1016/j.mcm.2011.11.076

[30] H. Aghayari, J. Nourinia, C. Ghobadi, and B. Mohammadi, "Realization of dielectric loaded waveguide filter with substrate integrated waveguide technique based on incorporation of two substrates with different relative permittivity," *AEU – International Journal of Electronics and Communications*, vol. 86, pp. 17–24, Mar. 2018. https://doi.org/10.1016/j.aeue.2018.01.008

[31] F. D. Q. Pereira, V. E. B. Esbert, J. P. Garcia, A. V. Pantaleoni, A. A. Melcon, J. G. L. Tornero, and B. Gimeno, "Efficient Analysis of Arbitrarily Shaped Inductive Obstacles in Rectangular Waveguides Using a Surface Integral-Equation Formulation," *IEEE Transactions on Microwave Theory and Techniques*, vol. 55, no. 4, pp. 715–721, Apr. 2007. https://doi.org/10.1109/TMTT.2007.893673

[32] R. Kushnin, J. Semenjako, Y. V. Shestopalov, "Accelerated Boundary Integral Method for Solving the Problem of Scattering by Multiple Multilayered Circular Cylindrical Posts in a Rectangular Waveguide," 2017 Progress In Electromagnetics Research Symposium – Spring (PIERS), St. Peterburg, Russia, pp. 3263–3271, May 2017. https://doi.org/10.1109/PIERS.2017.8262320

[33] C. Bachiller, H. Esteban, H. Mata, M. A. Valdes, V. E. Boria, Á Belenguer, and J. V. Morro, "Hybrid Mode Matching Method for the Efficient Analysis of Metal and Dielectric Rods in H Plane Rectangular Waveguide Devices," *IEEE Transactions on Microwave Theory and Techniques,* vol. 58, no. 12, pp. 3634–3644, Dec. 2010. https://doi.org/10.1109/TMTT.2010.2083951

[34] Trans Tech. Products for RF/Microwave Applications [Online]. Available: http://www.trans-techinc.com/files/tti_catalog.pdf [Accessed 12 Oct. 2018].

[35] EXXELIA TEMEX. Dielectric resonators 07/2015 [Online]. Available: https://exxelia.com/uploads/PDF/e7000-v1.pdf [Accessed 8 Oct.2019].

[36] M. Y. Sandhu and I. C. Hunter, "Miniaturized dielectric waveguide filters," *International Journal of Electronics,* vol. 103, issue 10, pp. 1776–1787, 2016. https://doi.org/10.1080/00207217.2016.1138531

[37] R. Snyder, "Practical aspects of microwave filter development," *IEEE Microwave Magazine*, vol. 8, no. 2, pp. 42–54, Apr. 2007. https://doi.org/10.1109/MMW.2007.335528

[38] J. Ossorio, V. E. Boria, M. Guglielmi, "Dielectric Tuning Screws for Microwave Filters Applications." *2018 IEEE/MTT-S International Microwave Symposium* – IMS, Philadelphia, PA, USA, pp. 1253–1256, June 2018. https://doi.org/10.1109/MWSYM.2018.8439857

[39] P. Harscher and P. Vahldieck, R. "Automated computer-controlled tuning of waveguide filters using adaptive network models," *IEEE Transactions on Microwave Theory and Techniques*, vol. 49, no. 11, pp. 2125–2130, Nov. 2001. https://doi.org/10.1109/22.963147

[40] RF Microwave. 5.8 – 11 GHz wide bandwidth band-pass filter, SMA female connectors [Online]. Available: https://www.rf-microwave.com/en/nbp/nmp/5-8-11-ghz-wide-bandwidth-band-pass-filter-sma-female-connectors/fbp-5.8-11g/. [Accessed 01 Nov. 2019]

[41] SAGE, Millimeter, Inc. 29 to 35 GHz Passband, 40 dB Rejection from DC to 27 GHz and 37 to 45 GHz, Ka Band, WR-28 Waveguide Bandpass Filter [Online]. Available: https://www.sagemillimeter.com/29-to-35-ghz-passband-40-db-rejection-from-dc-to-27-ghz-and-37-to-45-ghz-ka-band-wr-28-waveguide-bandpass-filter/ [Accessed 01 Nov. 2019].

[42] J. B. Ness and V. A. Lenivenko, "Design and manufacture of 'exact' waveguide filters," 2000 Asia-Pacific Microwave Conference Proceedings (Cat. No.00TH8522), 3–6 Dec. 2000, Sydney, NSW, Australia, pp. 507–511. https://doi.org/10.1109/APMC.2000.925884

[43] J. Zhou and J. Huang, "Intelligent tuning for microwave filters based on multi-kernel machine learning model," *5th IEEE International Symposium on Microwave, Antenna, Propagation and EMC Technologies for Wireless Communications*, 29–31 Oct. Chengdu, China, pp. 259–266, Dec. 2013. https://doi.org/10.1109/MAPE.2013.6689881

[44] V. Miraftab and R. R. Mansour, "Computer-aided tuning of microwave filters using fuzzy logic," *IEEE Transactions on Microwave Theory and Techniques*, vol. 50, no. 12, pp. 2781–2788, Dec. 2002. https://doi.org/10.1109/TMTT.2002.805291

[45] K. Kimsis, J. Semenjako, R. Kushnin, A. Viduzs, "A Numerical Implementation of Efficient Cross-section Method for the Analysis of Arbitrarily Shaped Dielectric Obstacles in Rectangular Waveguide," *2017 Progress in Electromagnetics Research Symposium - Spring* (PIERS), St. Petersburg, Russia, pp. 3937–3943, May 2017. https://doi.org/10.1109/PIERS.2017.8262320

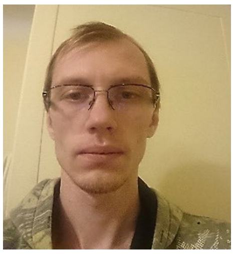

Karlis Kimsis received the B. sc. and M. sc. degrees in Electronics from Riga Technical University in 2014 and 2016, respectively. Currently he is a PhD student at Riga Technical University. His research interests include electromagnetic wave propagation and diffraction in waveguides and waveguide filters, especially tunable filters.

E-mail: karlis.kimsis@gmail.com

ORCID iD: https://orcid.org/0000-0002-5572-7106

Janis Semenjako is an Assistant Professor at the Department of Fundamentals of Electronics of Riga Technical University. He received the Dipl. Ing. degree in Radio Engineering in 1971 (Riga Polytechnic Institute – RPI), in 1976 he received a Dr. sc. ing. degree from RPI. From 1982 to 1983, he was a Research Fellow at the Faculty of EEI, Budapest University of Technology. His research interests include electromagnetic wave propagation and diffraction, guide-wave theory. The current interests include electromagnetic material characterization and uncertainty reduction, microwave filters.

E-mail: janis.semenjako@rtu.lv

ORCID iD: https://orcid.org/0000-0002-4961-2062

Yury V. Shestopalov received his M. sc. in Applied Mathematics in 1975 and Doctor of Science degrees in Mathematics and Physics in 1978 and 1988, respectively, from Moscow State University. In 1989, he was a postdoc at the Royal Institute of Technology and Stockholm University, Sweden. During the period of 1978–2000, he was an Assistant, Associate and Full Professor and Head of the Department at the Faculty of Computational Mathematics and Cybernetics and Kolmogorov School of Moscow State University. Since 2000, he has been an Assistant Professor and since 2008 – Professor in Applied Mathematics at Karlstad University, and since 2013 – at the University of Gävle. Yury Shestopalov has been active in several scientific fields, such as mathematical methods for electromagnetics, partial differential and integral equations, numerical methods, inverse problems, nonlinear analysis and various applications in electromagnetic field theory related to wave scattering, diffraction and propagation in linear and nonlinear media, investigation of materials, optics, contact mechanics, solution to large-scale problems with uncertain data, and supercomputer technologies. Among his scientific interests are also studies in didactics of applied mathematics. He is currently a Professor at the University of Gävle.

E-mail: yury.shestopalov@hig.se

ORCID iD: https://orcid.org/0000-0002-2691-282